

COLD ANTIHYDROGEN AT ATHENA:
EXPERIMENTAL OBSERVATION AND BEYOND * **

A. FONTANA^{a,b}, M. AMORETTI^c, G. BAZZANO^{a,b}, G. BONOMI^d, A. BOUCHTA^d
P. BOWE^e, C. CARRARO^{c,f}, C.L. CESAR^g, M. CHARLTON^h, M. DOSER^d
V. FILIPPINI^{a,b}, M.C. FUJIWARAⁱ, R. FUNAKOSHIⁱ, P. GENOVA^{a,b}
J.S. HANGST^e, R.S. HAYANOⁱ, L.V. JØRGENSEN^h, V. LAGOMARSINO^{c,f}
R. LANDUA^d, E. LODI RIZZINI^j, M. MACRÌ^f, N. MADSEN^{k,e}, G. MANUZIO^{c,f}
P. MONTAGNA^{a,b}, H. PRUYS^k, C. REGENFUS^k, A. ROTONDI^{a,b}, G. TESTERA^c
A. VARIOLA^c, AND D.P. VAN DER WERF^h

ATHENA Collaboration

^a Dipartimento di Fisica Nucleare e Teorica, Università di Pavia, 27100 Pavia, Italy

^b Istituto Nazionale di Fisica Nucleare, Sezione di Pavia, 27100 Pavia, Italy

^c Istituto Nazionale di Fisica Nucleare, Sezione di Genova, 16146 Genova, Italy

^d EP Division, CERN, 1211 Geneva 23, Switzerland

^e Department of Physics and Astronomy, University of Aarhus, 8000 Aarhus C, Denmark

^f Dipartimento di Fisica, Università di Genova, 16146 Genova, Italy

^g Instituto de Física, Universidade Federal do Rio de Janeiro

Rio de Janeiro 21945-970, Brazil

^h Department of Physics, University of Wales Swansea, Swansea SA2 8PP, UK

ⁱ Department of Physics, University of Tokyo, Tokyo 113-0033, Japan

^j Dipartimento di Chimica e Fisica per l'Ingegneria e per i Materiali
Università di Brescia, 25123 Brescia, Italy

^k Physik-Institut, Zurich University, 8057 Zürich, Switzerland

(Received October 28, 2003)

The experimental production and detection of cold antihydrogen atoms reported by the ATHENA Collaboration in 2002 represents a major step toward the study of the antiatom internal structure. The availability of a high number of antihydrogen atoms in a cryogenic environment is the key ingredient for a series of stringent tests of the CPT symmetry and of the gravitational weak equivalence principle that is foreseen on neutral antimatter. The experimental apparatus and the method used by ATHENA present some unique features that are first introduced. Then the absolute rate of antihydrogen production and the signal to background ratio in ATHENA are discussed, along with some preliminary results regarding the temperature dependence of antihydrogen production. Finally the future perspectives for laser spectroscopy of antihydrogen are briefly outlined.

PACS numbers: 36.10.-k

* Presented at the XXVII International Conference of Theoretical Physics, "Matter to the Deepest", Ustroń, Poland, September 15–21, 2003.

** Corresponding author: andrea.fontana@pv.infn.it

1. Introduction and motivations

The experimental test of fundamental symmetries at very high precision plays a major role in modern physics and in this context the CPT symmetry is of great interest. The CPT theorem holds for local fields in a Lorentz invariant, flat space-time and assures the invariance of a physical system under the simultaneous application of charge conjugation, space inversion and time reversal [1]. The consequences of this theorem for particles and antiparticles have already been verified in a series of impressive measurements of their respective properties: to date the highest relative precision measurements of the K^0 and \bar{K}^0 masses is of the order of 10^{18} , but is obtained with a model dependent method [2]. A new series of measurements is foreseen for the future on the simplest atomic state of neutral antimatter, the antihydrogen atom: the spectroscopic analysis of its internal structure and in particular of the $1S$ - $2S$ transition and of the hyperfine splitting in a magnetic field are expected to be a very stringent and direct high precision test of the CPT symmetry. Moreover, new and different theories not based on the assumptions of the CPT theorem [3, 4] allow for CPT violations and predict differences in the spectra of hydrogen and antihydrogen that could be detected [5] if a sufficient number of cold antihydrogen atoms is available.

The first observation of atomic antimatter in small quantities was performed in 1996 at CERN with a technique that allowed the formation of antihydrogen in flight by crossing a Xe jet target with the antiproton beam of LEAR: only 9 atoms were successfully detected [6]. A subsequent and similar experiment at Fermilab reported a slightly higher number of observations [7]. However both experiments created only a few antihydrogen atoms with kinetic energy in the range of 1–6 GeV, therefore not suited for high precision spectroscopy experiments that require antiatoms to be trapped at cryogenic temperatures. Low temperatures are needed for various reasons: first of all to maximize the production rate because the recombination cross sections expected to have a role in antihydrogen formation depend on negative powers of the temperature, but also to favor the trapping of the neutral antiatom that must have a low velocity. This has also the advantage of reducing the Doppler effect, which will be one of the factors determining the ultimate spectroscopic resolution of the future measurements.

The ATHENA experiment, operating at the new AD (Antiproton Decelerator) facility of CERN [8], exploited all these requirements and succeeded in the 2002 and 2003 runs in observing a large quantity of antihydrogen atoms at cryogenic temperature by mixing clouds of cold antiprotons and positrons within an electromagnetic trap [9]. Also the ATRAP collaboration, operating at CERN, subsequently reported antihydrogen observation with a similar production technique, but with a different detection system [10]. In

the following, the ATHENA apparatus, the technique used to produce and observe antihydrogen atoms and some preliminary results on the physics of antihydrogen will be illustrated.

2. Experimental apparatus and procedure

The ATHENA experimental apparatus [11] is comprised of four main subsystems (Fig. 1): the antiproton catching trap, the mixing trap, and the antihydrogen detector, which are located in a 3 T magnetic field, and a separate positron accumulator [12], with its own 0.14 T magnetic field. The traps, usually called Penning–Malmberg traps, consist of hollow cylindrical electrodes immersed in a coaxial magnetic field to confine charged particles axially and radially, respectively.

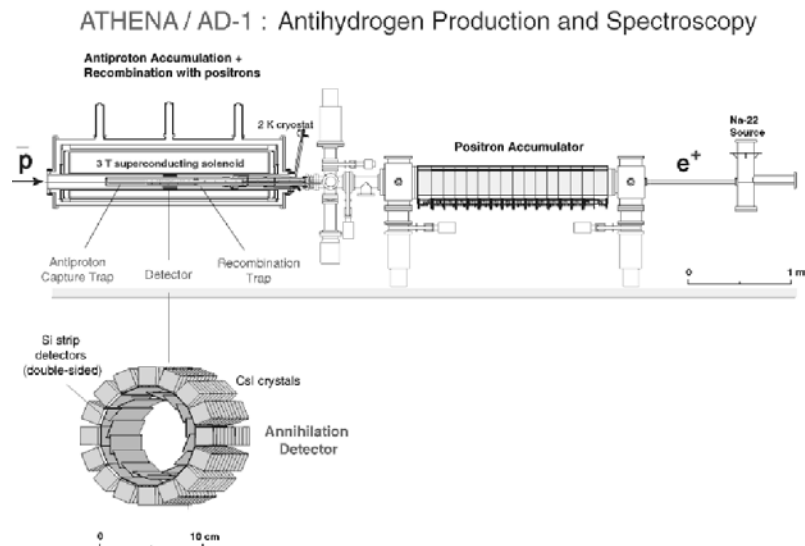


Fig. 1. Overview of the ATHENA experimental apparatus for production and detection of antihydrogen: below the main apparatus an expanded view of the antihydrogen detector is shown.

A cryostat (working at ~ 10 K) in the bore of the superconducting magnet surrounds and cools the catching and mixing traps, and forms an ultrahigh vacuum region.

Positrons are generated *in situ* via radioactive β^+ decay of a ^{22}Na source and are first moderated with a solid neon degrader and then cooled by collision with a nitrogen buffer gas in the positron accumulator. The accumulator is comprised of a series of sections with a differential pressure system that allows the stacking and storage of positrons with high efficiency: after about 2 minutes $\sim 1.5 \cdot 10^8$ positrons are transferred to the mixing trap with an

efficiency of about 50%; at equilibrium in the mixing trap these 75 millions positrons form a plasma of ellipsoidal shape [13]. Critical plasma parameters like radius, density, aspect ratio and temperature are monitored with a novel diagnostic technique that relies on the detection of oscillation modes [13].

The antiprotons are delivered from the AD facility in bunches of $\sim 10^7$ particles about every 90 seconds with a 5 MeV kinetic energy: these antiprotons, after passing through a degrader to reduce their energy to a maximum of 500 keV, are injected in the ATHENA catching trap where the low energy tail is trapped by using a high voltage switch. The trapped antiprotons are then cooled by Coulomb collisions with a cloud of electrons which is preloaded into the trap: the energy released is dispersed by the electrons via cyclotron radiation. After the electron cooling process, both the electrons and the antiprotons are at equilibrium with the cryogenic environment. The antiprotons are then transferred to the mixing trap with an efficiency between 50% and 100%.

In the mixing trap a potential well in a nested trap configuration [14] is formed to allow the confinement of the oppositely charged particles in the same space-time region and to facilitate their mixing.

When the two species of particles interact in this trap two processes occur: the antiprotons are first cooled by the positrons via Coulomb collisions, in a similar way to electron cooling, and then antihydrogen atoms are formed. These atoms, which are electrically neutral, are no longer confined in the nested trap and thus escape: the antihydrogen eventually collides with the trap walls giving rise to the simultaneous annihilation of both the antiproton and the positron. The antiproton–proton annihilation produces on average 3–4 pions, while the positron–electron annihilation produces two characteristic photons emitted back-to-back with energy of 511 keV. Both the pions and the photons are detected by an innovative detector designed to detect the space-time coincidence between the two annihilations (Fig. 2).

The antihydrogen detector, of 75 (140) mm inner (outer) diameter and 250 mm length, consists of a charged particle tracking detector in the form of two cylindrical layers of 16 double-sided silicon strip detectors ($160 \times 19 \text{ mm}^2$) each and of a photon detector in the form of a cylindrical array of 192 scintillating pure CsI crystals ($17 \times 17.5 \times 13 \text{ mm}^3$) read out by avalanche photodiodes. The trajectories of charged particles through the tracking detector are reconstructed as straight lines (with only two layers we do not reconstruct the curvature) and the antiproton annihilation vertex is determined by calculating the intersection between two or more tracks, with an uncertainty of 4 mm due to the straight line approximation. The photon detector measures the energies of low energy photons through the photo-conversion peak and is mainly sensitive to 2-photon decay, with an energy resolution of 24 % (FWHM) at 511 keV.

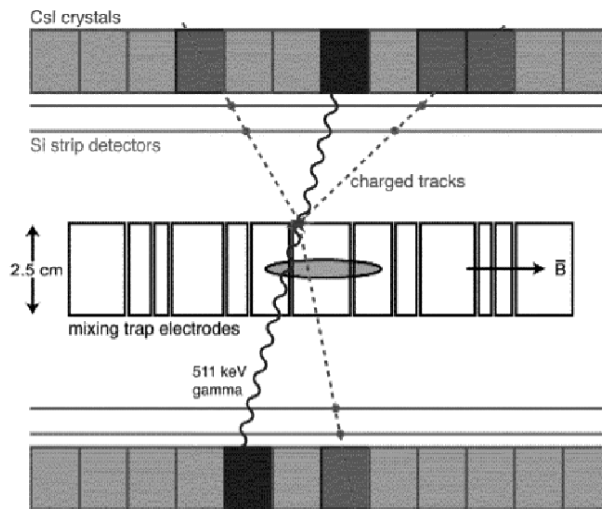


Fig. 2. The antihydrogen signature: the angle θ between the two emitted photons as seen from the annihilation vertex shows a peak at $\cos\theta = -1$ if the vertex and the two photons are collinear, indicating antihydrogen production. See text for details of the detector configuration.

Two types of mixing are used to study the recombination process: in standard conditions, the antiprotons are injected into the positron cloud with a relative energy of about 15 eV and allowed to mix for 180 s before they are ejected. We call this type of mixing ‘cold mixing’ because it happens at cryogenic temperature. A second type of mixing, called ‘hot mixing’, is obtained by exciting the axial motion of the positrons with a radio frequency signal applied to one of the mixing trap electrodes bringing the plasma to a temperature of several thousand Kelvin [13]: this results in a suppression of the production of antihydrogen and allows evaluation of the background component in the data and investigation of the temperature dependence of antihydrogen production. For the background study we also have a third type of mixing in which all the trapping and mixing sequences are executed in a harmonic trap without positrons: in this antiproton-only data set, no indications of antihydrogen production are expected.

3. Antihydrogen production

The data measured by ATHENA are believed to contain two components coming from different processes: antiproton annihilations on the rest gas, or on positive ions trapped together with the positrons, and antihydrogen annihilation on the trap walls. In our analysis [15], we used the two types

of mixing data (cold and hot) that contain the two processes in different proportions to estimate the absolute production rate of antihydrogen and the signal to background ratio. The hot mixing radial distribution shows an enhancement at small radii consistent with annihilations on the rest gas or on ions, while the cold mixing radial distributions shows an enhancement consistent with annihilation on the trap electrodes (radius 1.25 cm) as a result of antihydrogen formation.

An in-depth analysis has been performed to rule out any possible alternative mechanism in the antihydrogen identification by analyzing three experimental observables that can be used as indicators for antihydrogen: *(i)* the radial distribution of the annihilation vertices, *(ii)* the opening angle between the two photons as seen from the annihilation vertex and *(iii)* the trigger rate during the mixing cycle. The distribution of vertices are analyzed to determine the relative rates of the two components (antihydrogen and antiproton-only annihilation) by performing a 2-dimensional fit on the x - y distribution of the vertices for cold mixing in a fiducial volume ($z \in [-0.5, 1.5]$ cm) centered on the positron plasma (note that x and y are transverse to the axis of the magnetic field in the z direction). The data are fitted with a linear superposition of the experimental x - y distribution for hot mixing and by the Monte Carlo distribution for a pure antihydrogen sample (uniformly generated from $r = 0$ and $z < 1.5$ cm and isotropically emitted): the result (Fig. 3) gives an antihydrogen contribution of $(64 \pm 3)\%$. This result is in agreement with another fit which is performed on the 1-dimensional radial distribution: the data for cold mixing are interpolated with a function given by the linear superposition of the distributions for antiproton-only and for hot mixing data. The fit describes the cold mixing data as consisting of $(69 \pm 1)\%$ annihilations on the trap electrodes and of $(31 \pm 1)\%$ annihilations from background sources (*i.e.* consistent with events found during hot mixing).

The production of antihydrogen is also demonstrated by analyzing the distribution of the cosine of the opening angle: extensive Monte Carlo studies were performed before the data taking to take into account the effects of the electromagnetic showers in the magnet coils generated by the photons from the π^0 decay and indicated this angle as a crucial observable to experimentally identify antihydrogen (Fig. 4, left). The “golden events” of antihydrogen corresponds to $\cos \theta = -1$, *i.e.* to a perfect overlap between the vertex and the line joining the centers of two hit and selected crystals. Events characterized by $\cos \theta \neq -1$ can still correspond to antihydrogen atoms. This is due to various reasons: the additional bremsstrahlung photons that falls in the photopeak energy window around 511 keV, the low detection efficiency for these photons and the limited resolution on the vertex reconstruction. For these reasons the ideal topology of an antihydrogen

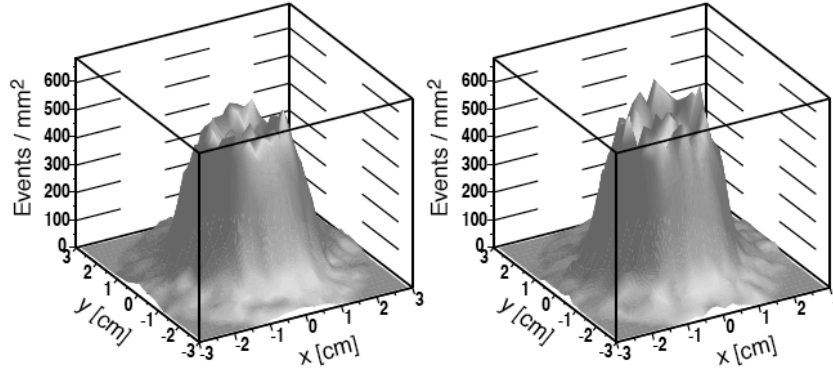


Fig. 3. x - y distribution of the reconstructed vertices in the fiducial volume for cold mixing (left) and result of the fit described in the text (right).

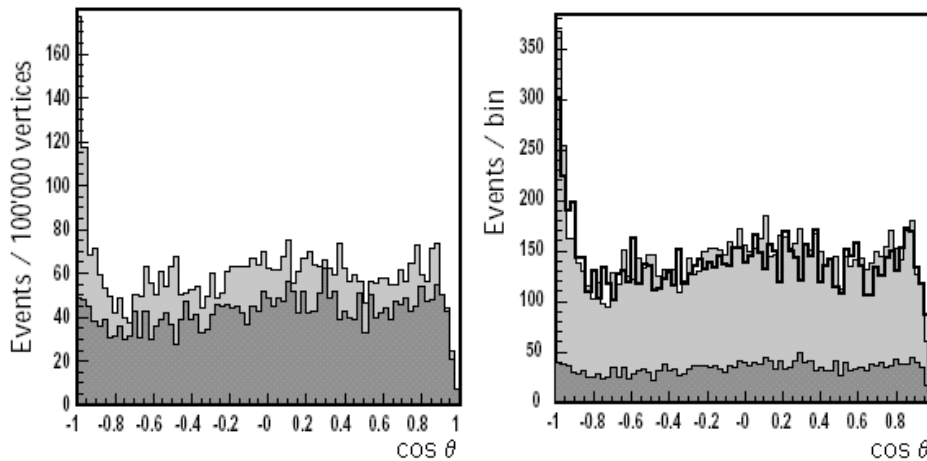


Fig. 4. Opening angle distributions: Monte Carlo predictions for the opening angle distribution in the case of a pure antihydrogen sample (left, light shaded) and of background antiproton-only annihilations (left, dark shaded area). Antihydrogen events generate the $\cos \theta = -1$ peak, but are also present in the plateau (see text). Same distribution for experimental data (right): the bold line represents data from cold mixing, the light shaded area is the prediction of the radial distribution fit and the dark shaded area is the contribution of the hot mixing data.

event is quite rare and a large fraction of antihydrogen events shows a random value of the opening angle. While pure antihydrogen shows this peak, the Monte Carlo data set for antiproton-only annihilations does not exhibit a peak: this prediction is in very good agreement with the experimental data (Fig. 4, right). As a further check for data consistency, we generated Monte Carlo events for the two components of the fits to the radial vertex distri-

butions normalized to the corresponding number of vertices and distributed the opening angle for these simulated data without any renormalization: the prediction from the radial distribution fit and the simulation is in very good agreement with the experimental observations. This supports our assumptions and indicates a fraction of $\sim (65 \pm 5)\%$ due to antihydrogen production. Also the study of the time evolution of the antihydrogen signals and of the detector trigger rates shows a difference between cold and hot mixing which is explained by antihydrogen production: the instantaneous trigger rate for cold mixing shortly after the beginning of mixing is ~ 300 Hz for 10^4 injected antiprotons and slowly decreases with time, while this behavior is not present for hot mixing.

In conclusion, our analysis indicates that in 341 cold mixing cycles in which 2.924×10^6 antiprotons have been injected in the mixing trap, about 494000 antihydrogen atoms have been produced: this correspond to an antihydrogen production efficiency of $\sim (17 \pm 2)\%$.

4. Temperature dependence

Two mechanisms are believed to play a role in the recombination process in ATHENA namely spontaneous radiative recombination and three-body recombination. In the first process a photon carries away the binding energy plus the kinetic energy of the positron in the center of mass frame, while in the second process the excess energy and momentum is carried away by a spectator positron. The two mechanisms predict a different dependence of the production rate on the positron plasma temperature: proportional to $T^{-1/2}$ for the two body process [16] and to $T^{-9/2}$ for the three body mechanism [17]. To study how the antihydrogen production is affected by the temperature it is possible to suppress formation by the application of a radio frequency excitation to the positron plasma, as was shown for the hot mixing data. ATHENA has the unique possibility of heating the plasma with different radiofrequency driving voltages and, for the first time, data were collected for different plasma temperatures ranging from no heating (corresponding to cold mixing) to ~ 3500 K (corresponding to hot mixing). The three observables introduced in the previous analysis show dramatic changes for different positron temperatures which can thus provide information concerning the production mechanisms. A clear decrease of the antihydrogen production with the temperature is indicated by our data, but a simple power law $T^{-1/2}$ or $T^{-9/2}$ or a combination of the two does not seem to fit the data [18]. The analysis is still in progress and a paper is in preparation, but new data and new theoretical work are also needed to completely understand the physics of the recombination process. What is clear is that antihydrogen production is still observed at room temperature and this is very important in the design in future experiments to produce antihydrogen.

5. Conclusions and future perspectives

This article briefly summarized the recent experimental results of the ATHENA collaboration that first succeeded in producing and observing cold antihydrogen atoms. The ability to produce a high number of cold antiatoms is necessary to perform laser spectroscopy: ATHENA is going in this direction by implementing laser stimulated recombination to maximize the antihydrogen yield and by making either a beam or by trapping the neutral antihydrogen to do spectroscopy. All these improvements will require time, but hopefully will facilitate new tests on fundamental symmetries and will bring the study of neutral antimatter to the deepest.

REFERENCES

- [1] J. Schwinger, *Phys. Rev.* **91**, 712 (1953).
- [2] J. Eades *et al.*, *Rev. Mod. Phys.* **71**, 373 (1999).
- [3] D. Colladay, *Phys. Rev.* **D55**, 6760 (1997).
- [4] J. Ellis *et al.*, *Phys. Rev.* **D53**, 3846 (1996).
- [5] R. Bluhm *et al.*, *Phys. Rev. Lett.* **82**, 2254 (1999).
- [6] G. Baur *et al.*, *Phys. Lett.* **B368**, 251 (1996).
- [7] G. Blanford *et al.*, *Phys. Rev. Lett.* **80**, 3037 (1998).
- [8] S. Maury, *Hyperfine Interact.* **109**, 43 (1997).
- [9] M. Amoretti *et al.*, *Nature* **419**, 456 (2002).
- [10] G. Gabrielse *et al.*, *Phys. Rev. Lett.* **89**, 213401 (2002).
- [11] M. Amoretti *et al.*, *Nucl. Instrum. Methods* **B**, in press.
- [12] D.P. van der Werf *et al.*, *Appl. Surf. Sci.* **194**, 312 (2002).
- [13] M. Amoretti *et al.*, *Phys. Rev. Lett.* **91**, 055001 (2003).
- [14] G. Gabrielse *et al.*, *Phys. Lett.* **A129**, 38 (1988).
- [15] M. Amoretti *et al.*, *Phys. Lett.* **B**, in press.
- [16] H.A. Bethe, E.E. Salpeter, *Quantum Mechanics of One and Two-Electron Atoms*, Plenum/Rosetta, New York 1977.
- [17] M.E. Glinsky *et al.*, *Phys. Fluids* **B3**, 1279 (1991).
- [18] G. Bonomi *et al.*, *Nucl. Instrum. Methods* **B** in press.